Title
The Impact of Air-Sea Coupling on Simulating SST Variability in the California Current System

Author
Walton, Daniel Burton

Publication Date
2012

Peer reviewed|Thesis/dissertation

UNIVERSITY OF CALIFORNIA

Los Angeles

The Impact of Air-Sea Coupling on Simulating SST Variability in the California Current System

A thesis submitted in partial satisfaction
of the requirements for the degree Master of Science
in Atmospheric Sciences

by

Daniel Burton Walton

2012

ABSTRACT OF THE THESIS

The Impact of Air-Sea Coupling on
Simulating SST Variability
in the California Current System

by

Daniel Burton Walton

Master of Science in Atmospheric Sciences
University of California, Los Angeles, 2012
Professor Alex Hall, Chair

Abstract

Here we show that air-sea coupling significantly impacts the simulation of sea surface temperature (SST) variability in the California Current System (CCS). Previous work has shown important differences between coupled and uncoupled models in simulating coastal SST, but only using empirical coupling or idealized scenarios. We compare the output of the UCLA Mesoscale Coupled Model to the output of a similar but uncoupled model over the CCS. These high resolution, realistic regional models have identical coastlines, bathymetry, and topography. They are forced at the boundaries by reanalysis data over the historical period 1981-1990. This model setup allows us to evaluate how including air-sea coupling impacts the accuracy of our simulation by comparing our model output to buoy observations. Both the spatial patterns and the amount of variability are more realistic in the coupled model, which is likely due to improved simulation of internal variability.

The thesis of Daniel Walton is approved.

Curtis Deutsch

James C. McWilliams

Alex Hall, Committee Chair

University of California, Los Angeles

2012

Contents

List of Figures

1 Introduction

Nearly 3 billion people live in coastal areas worldwide according to current estimates, and that number is expected to double to 6 billion as early as 2025 (Creel 1993). In California alone, 31 million people live in coastal counties, accounting for 87% of the population (Crossett 2004). Thus understanding the climate variability of coastal oceans has important consequences for millions of people. In this study, we focus on the variability of sea surface temperature (SST) in the California Current System (CCS).

SST is important because it regulates local atmospheric temperature, mesoscale winds, and other local weather phenomena such as fog and low clouds. Cold SSTs cools and increases the stability of the marine boundary layer, creating inversions. Cold SSTs can cause condensation and an inversion layer that prevents convection and traps moisture near the surface. This causes high relative humidity but low precipitation. SST gradients also alter mesoscale winds, having an effect on the same order as the coastal topography in shaping mesoscale wind anomalies (Boe et al. 2011).

SST in this region is modulated by a complex assortment of processes. Due to the location of the CCS on the eastern boundary of the North Pacific High, the CCS experiences primarily equatorward winds (which are especially strong in the summer due to strengthening of the North Pacific High). These winds force offshore Ekman transport of surface waters, causing upwelling of cold waters from the depths (Huyer 1983). The effects of upwelling are felt far from the coast as eddies, generated by instabilities in the coastal currents, contribute to cross-shore heat fluxes (Marchesiello et al. 2003). The intense coastal topography modifies these winds, creating strong gradients near capes and promontories, changing the shape and location of the upwelling regions (Enriquez and Friehe 1995; Boe et al. 2011).

Furthermore, SST anomalies alter the stability of the atmospheric boundary layer though heat fluxes, which alter the wind stress, forming an important feedback loop in this region (Chelton et al. 2007). Since colder SST leads to a more stable boundary layer, there is a reduced downward flux of momentum. The accompanying reduction of wind stress at upwelling locations alters the horizontal gradients and curls in the wind stress, altering nearby upwelling. This feedback loop

results in approximately linear relationships between wind stress curl and cross-wind SST gradients, and between wind stress divergence and down-wind SST gradients (Chelton et al. 2001; Maloney and Chelton 2006; Samuelson et al. 2006).

In addition to the forced variability due to large scale variation in the winds, there is also tremendous internal variability due to instabilities within the ocean itself. Research shows that realistic levels of eddy kinetic energy can be produced by forcing the ocean with only the mean seasonal cycle of heat flux and wind stress (Marchesiello et al. 2003). This demonstrates that variability in the atmospheric forcings is not necessary to create variability in ocean. Thus there are multiple important sources of SST variability, some due to changes in large scale atmospheric or oceanic conditions and some due to internal ocean processes.

Due to the intricacy of the coastline and topography, regional climate models with high resolution over a limited area are preferred to coarse resolution global climate models for modeling the CCS. In the past, studies have used regional ocean models that do not allow for feedbacks between the ocean and atmosphere. Because these models do not have a mechanism for SST to affect the atmosphere, they have no way to simulate important air-sea feedbacks. Thus recent research has attempted to create fully coupled ocean-atmosphere regionals models (Seo et al. 2007; Perlin et al. 2007, henceforth P07; Boe et al. 2011) or ocean models with empirical coupling (Jin et al. 2009, henceforth J09). By comparing with a similar uncoupled model, P07 and J09 show that during upwelling favorable times, coupling weakens wind stress, reduces upwelling near the coast, reduces the temperature anomalies and spreads them over a wider extent, due to enhanced offshore ekman pumping. J09 also demonstrated a reduction in eddy kinetic energy in the coupled model. (Neither Boe et al. 2011 nor Seo et al. 2007 compare their coupled results to uncoupled ocean models.) The work of P07 and J09 provides us valuable insights on the effects of coupling, but only in short, idealized coastline topography or with empirical coupling. In this study, we look to expand on this work by comparing a fully coupled regional model to an uncoupled model over the historical period 1981 to 1990 with high resolution, realistic topography. This work has the advantage of allowing a comparison between our model output and observations. Using measurements of SST taken at buoys along the coast, we can evaluate the effect of coupling on the accuracy of our simulation.

Because we want to see the effects of coupling on variability, we remove the mean seasonal cycle

from the model and observed SST. Furthermore, we ignore the inter-annual variability (oscillations with period greater than one year) since we have only ten years of model data available. This ten year period is too short to make robust statements about inter-annual modes of variability which we know can have time scales of years to decades. With multiple buoys not taking measurements until 1982, there is much less coverage for the first part of the 1981-1990 period. This should not affect our ability to compare the high frequency modes of variability, which will have multiple cycles, but it makes it difficult to compare lower frequency modes to observations. Hence we narrow this study to intra-annual variability, which we define as oscillations with period less than one year.

In Section 2, we present the setup for the coupled and uncoupled models and introduce the buoy observations. Next, in Section 3, we do a validation of the two models' mean SST, showing that models have a realistic base state, before moving on to variability in Section 4. In Section 4, we start by assessing the magnitude of the modelled variability to see if the models have the right amount of variability. Then we use correlation to assess which model is in better phase agreement with observations. Next we compare the spatial patterns of coherent variability in each model to observations. We then split the intra-annual variability into high and low frequencies to reveal where most of the discrepancies between the two models lie. In Section 5, we discuss the implications of our results and the sensitivity of our results to our domain configuration. We draw conclusions about the importance of coupling in Section 6.

2 Data

2.1 Regional Ocean Simulations

The simulated data for this study consists of daily average SST from two regional ocean models run over the period 1981-1990. The first is the UCLA Mesoscale Coupled Model (UMCM; see Boe et al. 2011). The UMCM couples the Advanced Research Weather Research and Forecasting (WRF) atmospheric mesoscale model to the Regional Ocean Modeling System (ROMS) ocean model. WRF (Skamarock et al. 2007) is a community model that contains a fully compressible non-hydrostatic dynamical core with a run-time hydrostatic option and full physics suite. To simulate land-surface processes, WRF is equipped with the NOAH Land Surface Model (Chen and Dudhia 2001). The

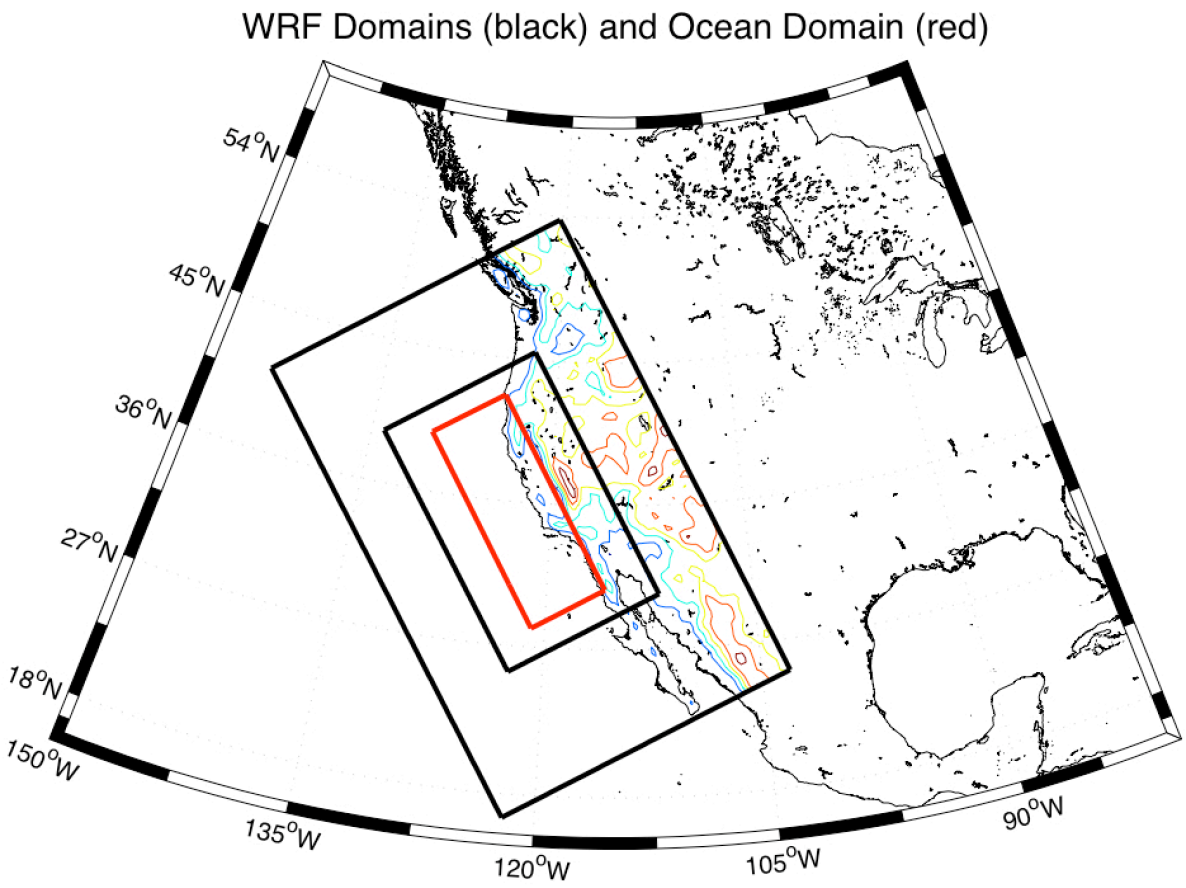

Figure 1: WRF 36 km and 12 km resolution domains (black), ROMS 4 km domain (red), and topography (colored contours).

parameterization schemes used in this study are the Yonsei University Scheme for the planetary boundary layer (Hong et al. 2006), the WRF Single-Moment 3-Class Scheme for microphysics, the Rapid Radiative Transfer Model for longwave radiation (Mlawer et al. 1997), and the Dudhia Scheme for shortwave radiation (Dudhia 1989).

The ROMS regional ocean model (Shchepetkin and McWilliams 2005, 2009) solves the hydrostatic, free-surface primitive equations in 3D curvilinear coordinates that follow the bottom orography and sea level exactly and the coastline approximately. ROMS uses accurate algorithms for preserving the extrema, pressure gradient force, compressible sea-water equation of state, and split-explicit time-stepping for simulating the barotropic and baroclinic modes. Multiple studies have successfully validated ROMS in coastal areas with strong upwelling (Marchesiello et al. 2003; Seo et al. 2007; Capet et al. 2004, 2008).

The UMCM is configured to simulate the atmospheric and oceanic variability in the area surrounding the coast of California. It uses two nested WRF domains of 36 km and 12 km resolution, and a single ROMS domain with 4 km resolution (Figure 1). The lateral atmospheric boundary conditions come from the North American Regional Reanalysis data set (NARR) at 32 km resolution, interpolated to 36 km resolution to match the outer WRF domain. The lateral oceanic boundary conditions are output from a slightly lower resolution 5 km ROMS run. The lateral boundary forcing for this 5 km ROMS run comes from the Simple Ocean Data Assimilation (SODA) dataset (Carton et al. 2008).

The WRF and ROMS models are only coupled in the ROMS domain. To couple the two component models, WRF sends two-hour averaged wind stress, surface heat and water fluxes to ROMS at two-hour intervals. One hour after ROMS receives the WRF data, ROMS sends the two-hour averaged SST. The first model is referred to as the *coupled model*. The second model is intended to simulate the ocean when the air-sea coupling is disabled and is referred to as the *uncoupled model*. The uncoupled model has the same WRF and ROMS domains and the same lateral boundary conditions, but there is no coupling in the ROMS domain. Instead, we use the 5 km ROMS run as the surface forcing for the WRF model. Then the 12 km WRF output is used to force 4 km ROMS at the surface. Thus the ocean to atmosphere feedback from 4 km ROMS to 12 km WRF has been removed.

2.2 Buoy Observations

To compare our two ocean runs with reality, we use the hourly SST measurements from ten moored buoys off the coast of California operated by the National Data Buoy Center (NDBC). Locations of these buoys are shown in Figure 2. Four of the buoys began recording SST in 1981, four more began in 1982, and the final two began in 1983. Figure 3 shows the data availability for the buoys during the period January 1981 through December 1990. Although there is enough data over this period for analysis, there are many missing data, up to 30% at some buoys.

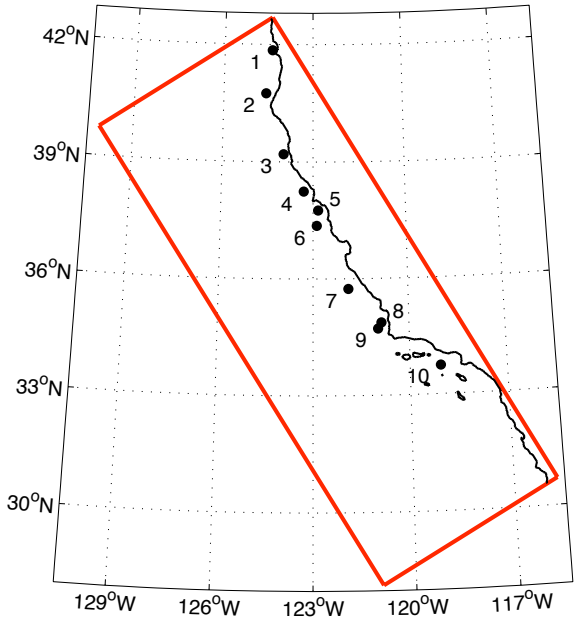

Figure 2: Locations of the NDBC buoys used in our model validation. The ROMS 4 km domain is in red.

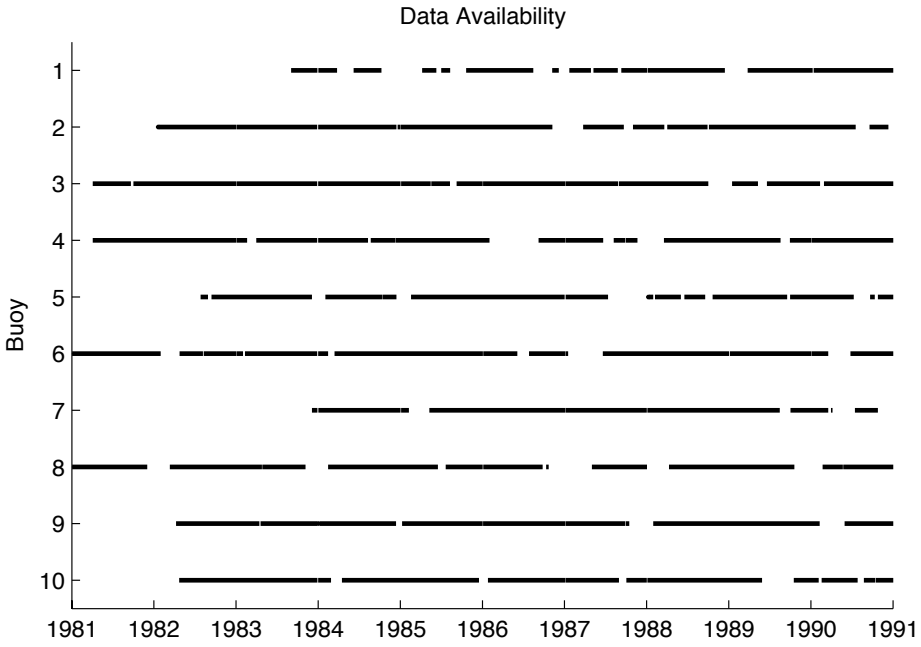

Figure 3: Data availability for SST measurements at the NDBC buoys. Black lines indicate periods where measurements are recorded and open spaces indicate temporal gaps in the data.

3 Validation of Mean SST

Prior to analyzing SST variability, we demonstrate that both models accurately simulate the mean state. Figure 4 shows the annual mean SST for the coupled run, uncoupled run, and observations. The two models have similar mean SST fields. Both have a strong coastal cold band, especially along the northern California coast, where upwelling (primarily in the summer) brings cold water to the surface. The two models clearly reproduce the southward increase in temperatures present in the observations. Even the small differences in temperature between nearby buoys (for instance Buoys 4 versus Buoy 6) are captured by the models. The strong correlations of 0.97 (0.98) between observed mean SST and the values at the closest model grid points of the coupled (uncoupled) model values show that the models properly represent the observed spatial pattern. The one region where the models do not perform as well is near buoy 10 in the Southern California Bight (SCB). This may be due to the intense coastal topography in the SCB and the presence of the Channel Islands. Dong et al. (2011) have shown that increasing resolution and adding tides in this region may be necessary for accurate simulations. Overall, Figure 4 gives us confidence that both models accurately simulate the mean SST.

4 Comparing Intra-Annual SST Variability of Model and Observed Time Series

In this Section, we compare the observed intra-annual SST variability measured at the buoys to simulated variability. To perform this comparison, we start with the observed time series from each buoy and the simulated time series at the model grid point nearest to each buoy. Then we remove the seasonal cycle from each of the time series. The mean seasonal cycle is calculated by taking the ten-year average for each day of the year and then fitting the result with three harmonics with periods of one year, six months, and four months. Because the seasonal cycle of SST in this region is not a perfect sine wave, we need at least three harmonics to reasonably fit the seasonal cycle. If we use more than three harmonics, the seasonal cycle begins to incorporate higher frequency oscillations that are due to transient forcings, rather than the climatological seasonal forcings. After

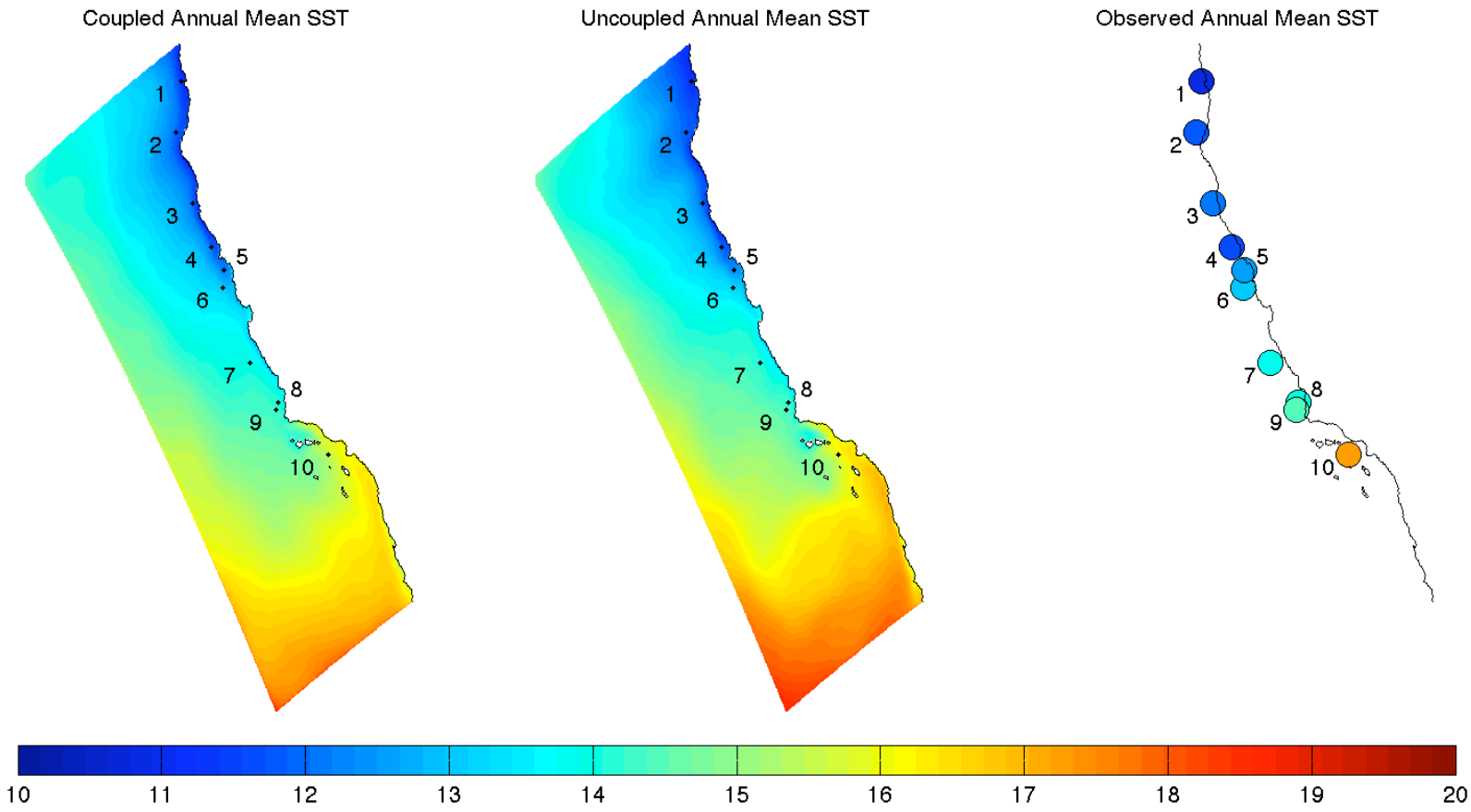

Figure 4: Annual mean SST for the coupled run, uncoupled run, and observations.

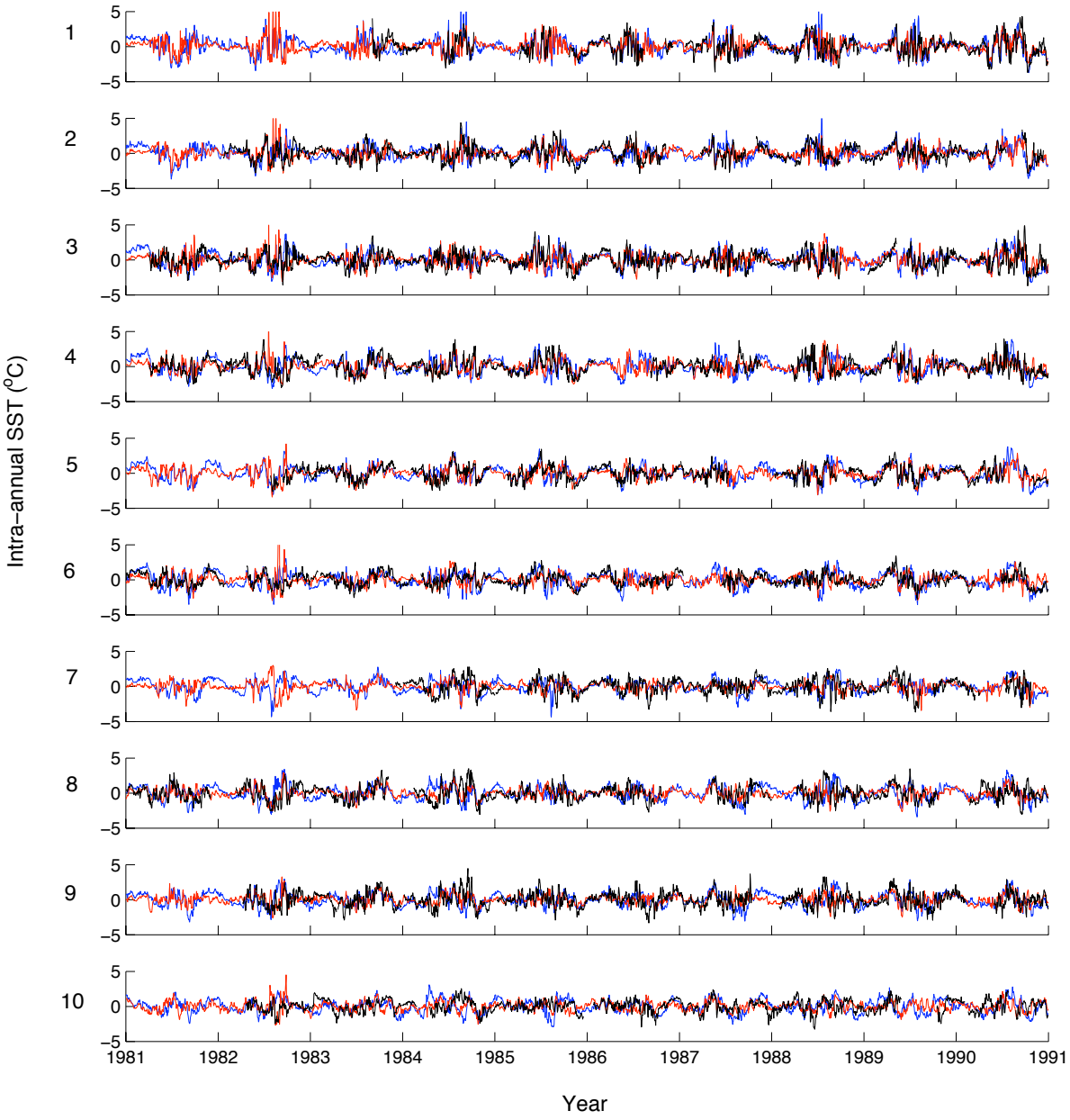

Figure 5: Intra-annual SST time series for the coupled run (blue), uncoupled run (red), and observations (black). Buoys are ordered from north to south, with Buoy 1 at the top and Buoy 10 at the bottom.

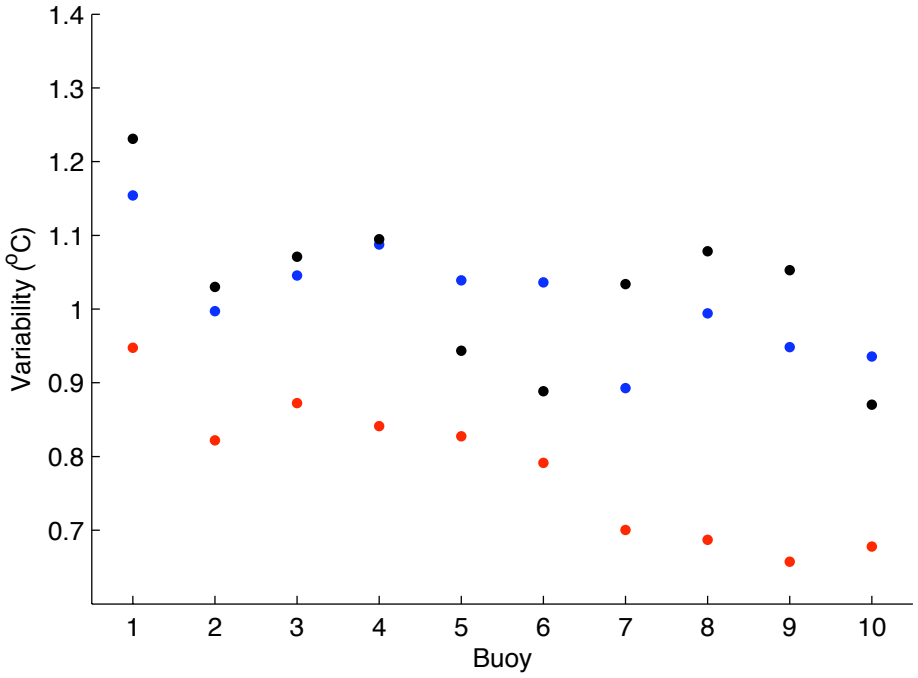

Figure 6: Amount of intra-annual SST variability at the ten buoy locations for the coupled model (blue), uncoupled model (red), and observations (black). Variability is calculated as the standard deviation, σ, of the time series. The uncoupled model consistently underestimates the variability along the coast.

the seasonal cycles are subtracted from the time series, a high pass filter is applied to remove all of the interannual variations (harmonics of period greater than 365 days). With the mean seasonal cycle and the interannual variations removed, the remainder is the intra-annual time series, shown in Figure 5. There is a clear seasonal pattern of increased variability during the summer upwelling season and a decrease in variability during the winter. This seasonal pulsing of the variability is visible at nearly all locations for both the models and the observations. The pulsing is most likely due to variability in the equatorward winds that cause upwelling, which are stronger in the summer. However, there is clearly variability at all times throughout the year, which may partly reflect the passage of winter storms or oceanic mesoscale eddies and filaments.

4.1 Magnitude of Variability

First, we compare the amount of intra-annual variability in the models to observations at the ten buoy locations. To quantify the variability at a location, we use the standard deviation, σ, of the intra-annual time series. (For the observational time series, we ignore days where there are no observations.) This quantity is shown in Figure 6, for each location. There is uniformly more variability in the coupled model (average = 1.0 °C) than the uncoupled model (average = 0.8 °C). The level of coupled variability is also much closer to observations (average = 1.0 °C) at all buoys but one. The uncoupled model systematically underestimates the variability especially at Buoys 7-10. Overall, the coastal variability levels in the coupled model are much more realistic.

4.2 Phasing of Variability

Next, we correlate the model time series with observations (Figure 7, blue and red dots). The correlations are significantly less than one at all locations and especially low at the southern buoys. The uncoupled model SST is slightly better in phase with observations (mean correlation = 0.51) than the coupled model (mean correlation = 0.41).

Low correlations may not be an indication of poor model performance. Instead, low correlations may indicate large amounts of internal variability in this particular region. Internal variability (variations arising from internal ocean instabilities that are not in response to external forcings) is common in the CCS in the form of eddies and filaments (Marchesiello et al 2003). We expect that ocean's internal variability, should be randomly phased between each model and the observations. In contrast, we would expect the forced variability (the response to external forcings) to be largely in phase between the observations and our models. The two models share the same boundary conditions, so they should have the same forced response, except in the ways that coupling alters that response. Futhermore, since reanalysis boundary conditions are our best estimate of reality, we also expect each model's forced response to be in phase with observations. However the forced variability of the models may not be in phase with observations, if the models are unrealistic. Thus low correlations have two principal causes: internal variability and poor model realism.

In our study these low correlations are due to the presence of internal variability. If our models

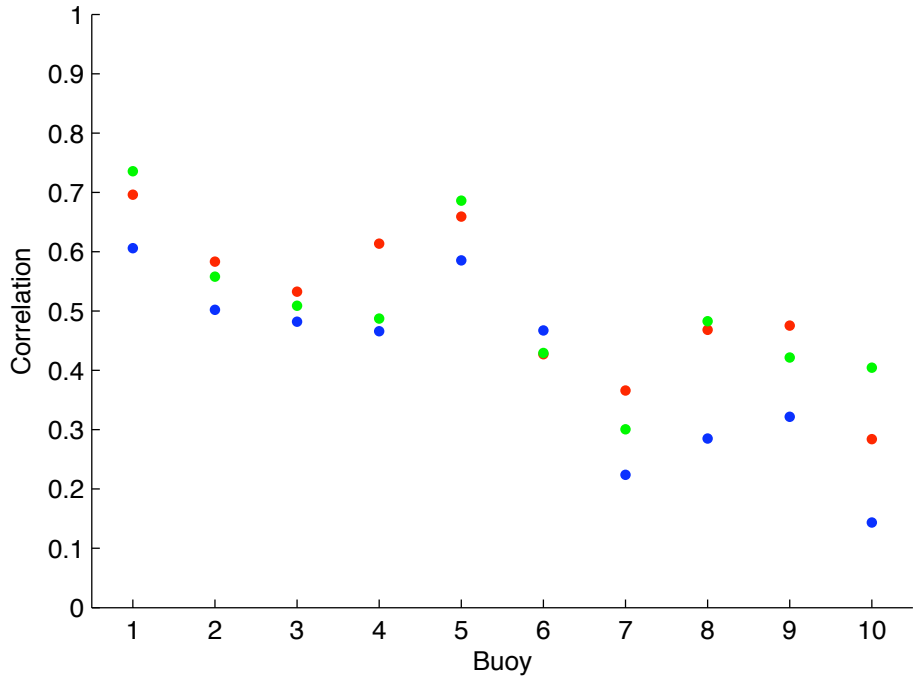

Figure 7: Correlations at each of the ten buoy locations. Shown are the correlations between coupled model and observations (blue), uncoupled model and observations (red), and coupled and uncoupled models (green). Note the correlations are slightly higher for the uncoupled model than for the coupled model. At buoys with low correlations between the models and observations, the correlation between the models is also low.

were unrealistic and had no internal variability, correlations between models and observations would be low and inter-model correlations would be high (though not perfect, because of the differences due to coupling). However, this is not the case. Inter-model correlations (Figure 7, green dots) closely mirror the correlations between models and observations (red and blue dots). While this could be explained if the differences due to coupling (which cause inter-model differences) happened to be the exact same size as the differences due to lack of model realism (which cause model-observation differences), this is unlikely. A simpler explanation is the influence of internal variability, which is present in different amounts at the different buoy locations. Buoy locations with lower correlations have proportionally more internal variability (or less forced variability) than locations with higher correlations.

Since inter-model correlation is a reasonable proxy for the ratio of forced to internal variability,

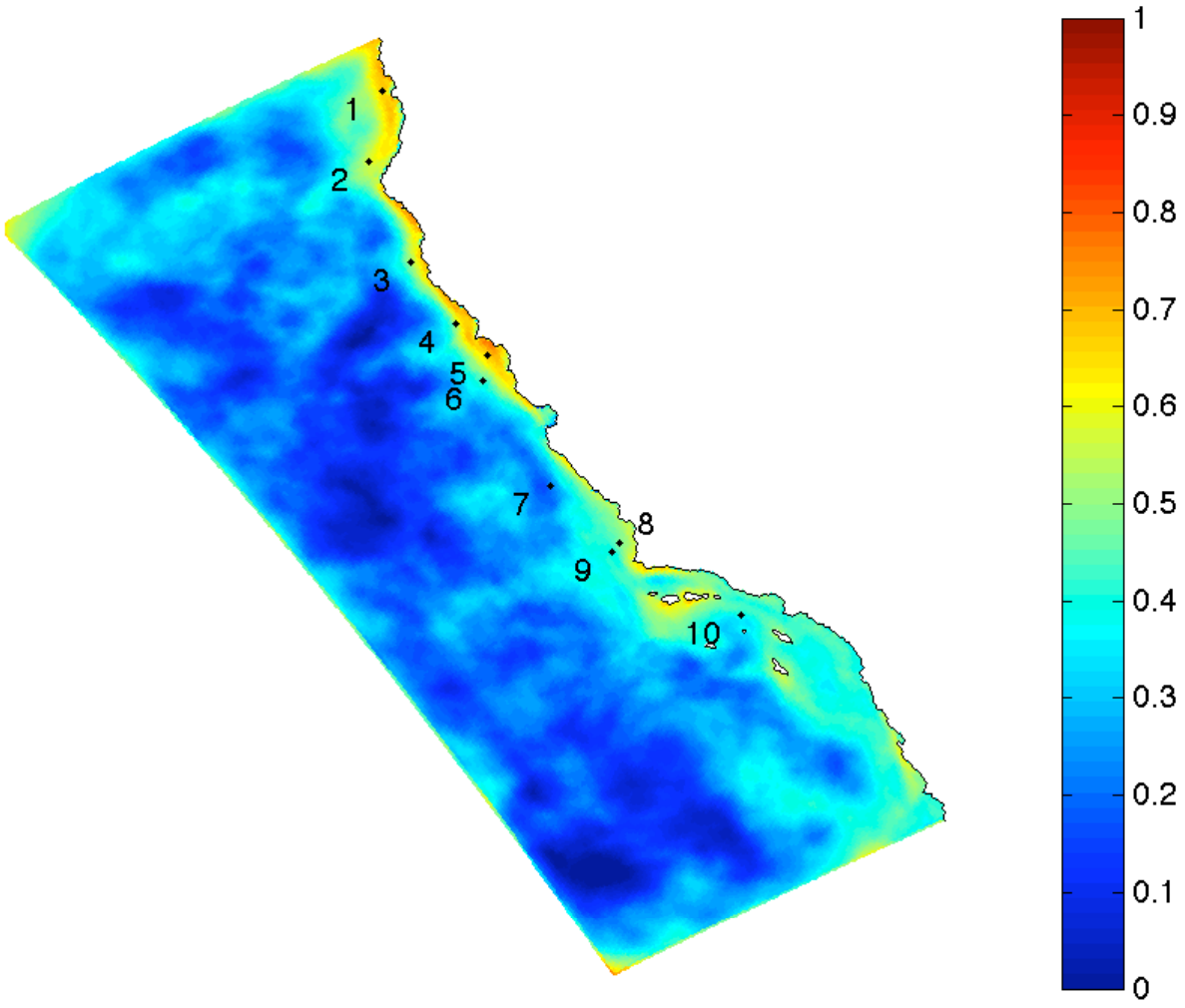

Figure 8: Correlation between coupled and uncoupled intra-annual SST. The highest correlations are along the coast, especially downwind of the capes and promontories. Boundary effects are also visible. These are somewhat higher correlations within the first three to five model grid points from the domain edge. We expect any near-boundary points to have artificially high correlations, since the boundary conditions are the same for the two models.

we calculated the inter-model correlation at each grid point in our domain to determine the relative prevalence of internal variability (Figure 8). There is a stark contrast between the regions of predominantly forced variability near the coast, where correlations reach 0.7 or higher, and the open ocean, where correlations are less than 0.4 and internal variability dominates.

The highest correlations are found in narrow strips on the lee side of the capes, promontories, and islands, which consistent with the work of Enriquez and Friehe (1995) and Marchesiello et al. (2003). The northern coast may have especially strong upwelling because the coastline is most parallel to the equatorward winds. Since the wind anomalies generating upwelling come from the WRF boundary conditions and pass through our model domain on the time scale of days, the phasing of these anomalies is nearly identical in the coupled and uncoupled simulations. Thus the simulations have similar phasing of variability due to wind-driven upwelling. Most buoy locations lie within the these coastal upwelling zones.

In contrast, open ocean correlations are much weaker. This suggests that the ratio of forced to internal variability is lower here. Away from the coastal zones, upwelling is less prevalent, so the forced signal is reduced. Eddies and upwelling filaments are also present, especially during the summer months (Marchesiello 2003). Because the propagation of anomalies in the ocean is much slower than in the atmosphere (on the order of weeks), there is ample time for instabilities to develop and modify the signals from the boundary forcing as they make their way to the interior. These eddies and filaments are due to nonlinear instabilities, so we expect them to be randomly phased between the coupled model, uncoupled model, and observations. Thus lower correlations with observations here would be expected, even in a perfect model.

Reexamining Figure 7, we can understand the variations in correlation from buoy to buoy by putting them in context of Figure 8. Because the regions of forced variability due to coastal upwelling are narrow, the correlations are highly sensitive to the exact location of the buoy. For instance, there is a big difference between the correlations at Buoys 4 and 6, even though they are relatively close. Buoy 4 lies right in the zone of high correlation between the coupled and uncoupled models, while Buoy 6 is just outside this narrow strip. Presumably this is an indicator that Buoy 4 is generally within the upwelling zone, while Buoy 6 is not. Looking at Figure 7, it would be tempting to conclude that there is an increase in model performance with latitude. However, the

upwelling strengthens as you go north, so this may be an indication of increased forced variability with latitude.

4.3 Spatial Structure of Coherent Variability

Due to the presence of internal variability in the CCS, correlation is an incomplete measure of model performance. As we saw above, high correlations with observations indicate both that a large fraction of the variability is forced and that the forced variability has a realistic phasing. However, a good model must also simulate the spatial structure of the variability. We have already seen that the coupled model performs better at simulating the amount of SST variability. Now we investigate which model has more realistic spatial structure of variability.

To examine the spatial structure of the variability, we require a metric that reveals which regions have shared variations. We define the pattern of coherent variability (relative to a grid location P) to be the map of correlations between P and all other grid points for that model. The pattern of coherent variability tells us which areas have variability that is well correlated with P. By our definition, coherent variability can be either forced or internal. For instance, a surge in the strength of summertime equatorward winds due to external forcings may increase upwelling and cause a decrease in temperature simultaneously along the entire coast. On the other hand, a drop in temperatures due to a large cold eddy that started near Buoy 8 may also have a similar signature at Buoys 7 and 9.

An example of a pattern of coherent variability relative to grid point nearest Buoy 8 can be seen in Figure 9. This shows the pattern first for the coupled model (a) and then for the uncoupled model (b). There is a dramatic difference between the two models' patterns of coherent variability. In the coupled model, correlations above 0.5 are present along the entire coast and as far as 300 km from shore. In contrast, for the uncoupled model, the region of correlations above 0.5 is isolated within 150 km of Buoy 8 with only a narrow sliver less than 50 km wide extending up the Central Coast. When the procedure is repeated for each of the other nine buoys locations, the coupled spatial patterns are always stronger and broader.

To evaluate which model has more realistic coherent variability patterns, we compare the coupled and uncoupled coherent variability to observations, but sample only at the buoy locations. In

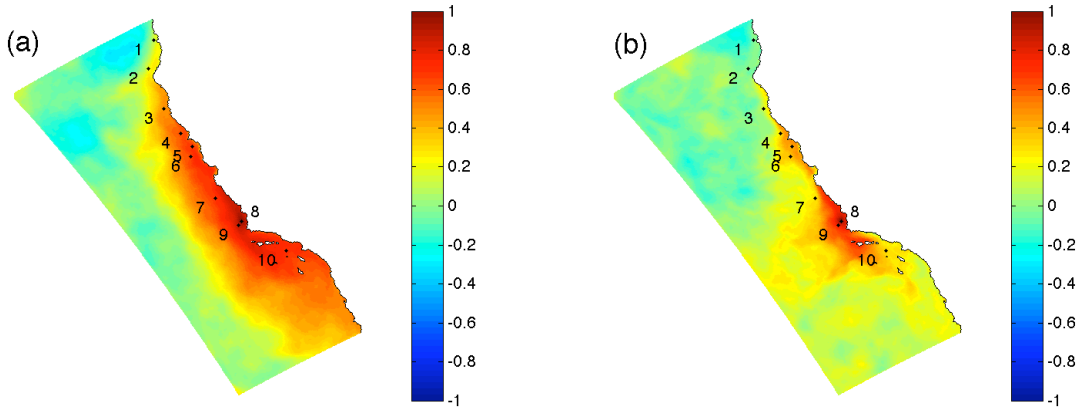

Figure 9: Correlations of intra-annual SST between the model grid point nearest Buoy 8 and every other point in the domain for (a) the coupled run and (b) the uncoupled run.

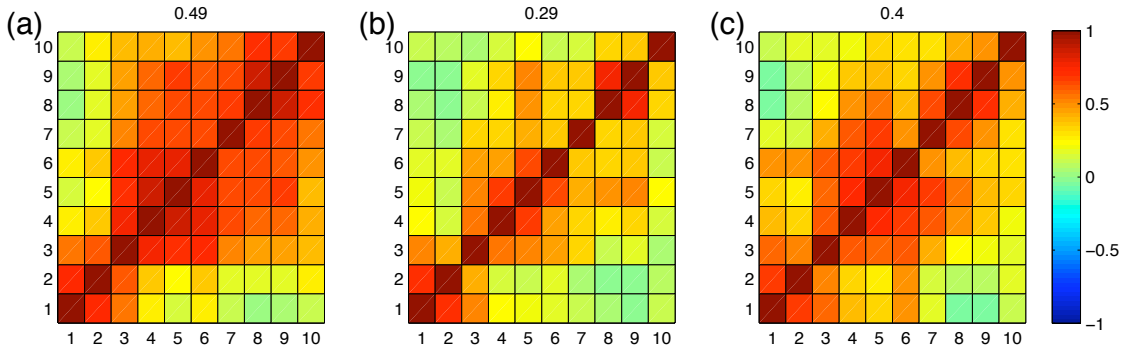

Figure 10: Correlations of intra-annual SST between each pair of buoy locations for (a) the coupled run, (b) the uncoupled run and (c) observations. Mean correlations (averaged over all non-diagonal entries) are above each plot.

other words, we calculate the correlation of the time series for each pair of buoy locations. This method of evaluation will tell us how far up and down coast the shared signals generally occur, but because we have no buoy observations far from the coast, we cannot verify the width of the patterns. Figure 10 shows the correlation between the intra-annual SST at each buoy location in (a) the coupled run, (b) uncoupled run, and (c) observations. By comparing panels (a) and (b) we see that the patterns of coherent variability are much weaker in the uncoupled model at all buoy locations, not just the location of Buoy 8. The average correlation between distinct buoy locations in the coupled run is 0.49, significantly greater than 0.29 for the uncoupled run. The average for the observations was 0.40, which is slightly closer to the coupled average. Since random sampling error in the observations will act to artificially reduce the observed correlations, the actual correlations may be even closer to the coupled values.

There are two possible causes for these differences in coherent variability. First, air-sea interaction may allow the atmosphere to spread temperature anomalies to distant locations. Temperature anomalies in the ocean can be transmitted to the atmosphere in the coupled model, and since winds typically travel faster than ocean currents, they can be retransmitted to the ocean at more distant locations. However, this effect is limited by the low heat capacity of air relative to water.

A second possibility is that air-sea coupling may protect anomalies, allowing them to persist longer. The work of P07 shows that when comparing a coupled ocean atmosphere system to one with a unchanging atmosphere, the coupled system has lower heat flux. Because a coupled atmosphere is allowed to cool (warm) above a cold (warm) ocean anomaly, the atmosphere will reduce its heat exchange from the ocean, allowing the anomaly to persist longer. This process should preferentially affect internal variability over forced variability. Recall that for the uncoupled model, 5 km ROMS forces 12 km WRF, which then forces 4 km uncoupled ROMS. If a particular anomaly is forced, then we suspect that the 5 km ROMS would share that anomaly with the the 4 km uncoupled ROMS. In that case, the atmosphere in 12 km WRF run would have evolved appropriately, as if it was coupled. In contrast, if an anomaly is the result of internal variability, it is likely to be out of phase with the 5 km run and thus also out of phase with the 12 km WRF forcing.

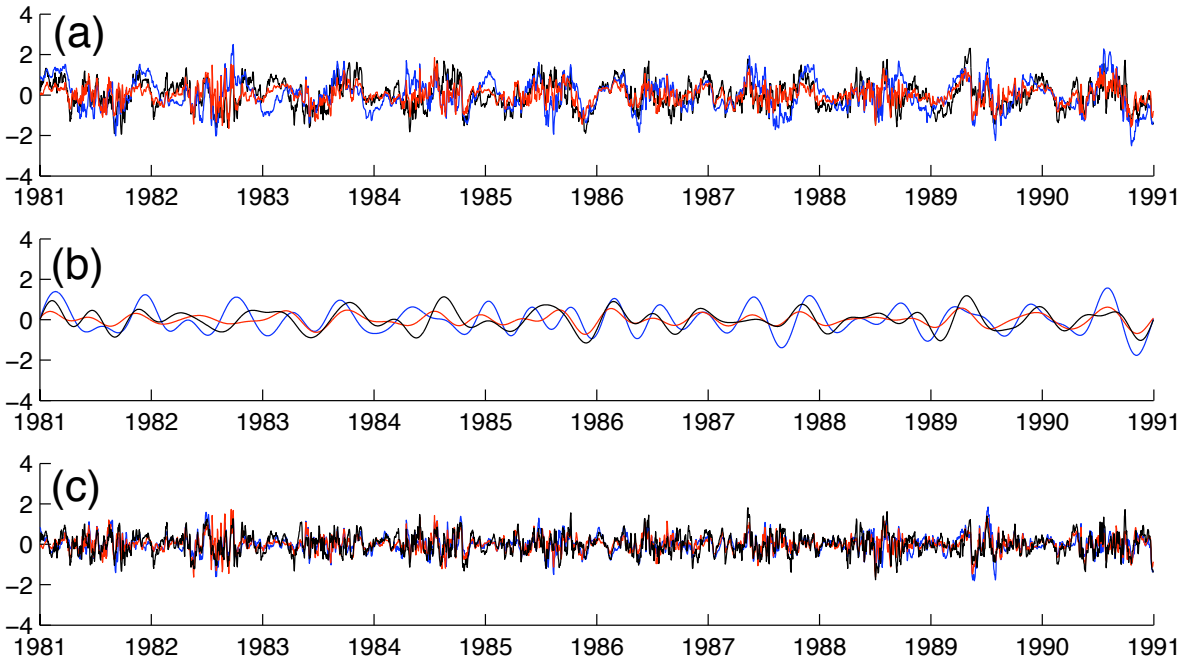

Figure 11: Plotted in (a) are the coastal mean time series for the coupled run (blue), uncoupled run (red), and observations (black). Plotted in (b) is the coastal mean time series after low pass filtering (periods greater than 120 days). Plotted in (c) is the coastal mean time series after high pass filtering (periods less than or equal to 120 days).

4.4 Time Scales of Coherent Variability

Separating the time scales of coherent variability reveals that differences between the two models are largest at lower frequencies. In order to perform this comparison, we create the coastal mean time series, which is the average time series over all ten buoy locations. By averaging over all of the buoy locations, the coastal average is an estimate of the variability shared by all of the buoys locations. We also created the coastal mean time series for the observations. Buoys with no available data for a given day were not used to compute that day's observed coastal mean. For each day over the ten year period at least one buoy is available, so the coastal average does not have any missing days, unlike the time series at the individual buoys.

The coastal means for the coupled model, uncoupled model, and observations are plotted in panel (a) of Figure 11. There is significant agreement among the three coastal mean time series

($r > 0.45$ between each pair), indicating that much of the variability shared among the buoy locations is common to the two models and observations. But large differences between the three time series are also visible. Much of the disagreement is in the lower frequency oscillations. Panels (b) and (c) of Figure 11 show the coastal mean after subjecting it to low pass and high pass filters, each with a cut off period of 120 days. There is much better agreement between the high pass series than the low pass series. The correlation between the two models are 0.73 for the high pass and only 0.55 for the low pass. Since we believe that the inter-model correlation is a good proxy for forced variability, this indicates significant forced variability at both time scales, but relatively more forced variability at higher frequencies.

In addition to differing in phase at low frequencies, the two model coastal means also differ in magnitude. Using standard deviation to measure the magnitude of the low pass variability as above, we find the coupled model has a standard deviation of 0.63 °C, more than twice that of the uncoupled model's 0.27 °C. This large difference in variability is visible in panel (b) of Figure 11. The observed low pass variability is between the models at 0.49 °C. The presence of internal variability could explain the low correlations, but not the differing amount of variability. Therefore, the coupling must be responsible for the increased variability.

Although we have limited this paper to intra-annual variability so far, it is interesting to note that the interannual and seasonal variability are also larger in magnitude for the coupled model. While we only have ten years of data, which is too small of a sample for many of the long time scale modes of variability like El Nino Southern Oscillation or the Pacific Decadal Oscillation, there is a clear difference in the magnitudes of the coupled and uncoupled models. The average interannual variability over the buoy locations is 0.86 °C for the coupled model and only 0.42 °C for the uncoupled model (significantly different at the $\alpha = 0.05$ level). Similarly, the mean size of the seasonal cycle in the coupled model is 1.44 °C compared to 1.06 °C for the uncoupled model (significantly different at the $\alpha = 0.05$ level). This further supports our claim that coupling has strong effects on the variability, especially on longer time scales.

5 Discussion

Based on the work of P07 and J09 we would expect the coupled run to show weaker and more diffuse upwelling and reduced eddy kinetic energy, leading to decreased SST variability. Instead we see stronger SST variability in the coupled run. We believe this is due to the differences between their uncoupled model configuration and ours. In the idealized scenarios of both P07 and J09, the uncoupled atmosphere was held constant and not allowed to receive any information from the ocean. In our case, the uncoupled WRF run was forced by SST from the ROMS 5 km run. Thus the uncoupled WRF run incorporates a response to the ROMS 5 km run. Since we expect the ROMS 5 km run and the uncoupled ROMS 4 km to have similarly phased forced variability but randomly phased internal variability, we expect the uncoupled WRF run to incorporate a response to the forced variability of ROMS 4 km run, but not to its internal variability. Thus we expect to see more of a difference between our coupled and uncoupled model in the treatment of internal variability. In Section 4.4, for the coastal mean time series, the longer time scale variability not only had weaker correlations between the models and observations - an indication of internal variability - but also the magnitude of the variability was much different between the two models. The coupled low frequency variability was more than twice the uncoupled magnitude. This is evidence that coupling disproportionately affects the internal variability.

Our results showing stronger variability in the coupled model are not actually in conflict with previous studies. Because of the differences in experimental setup, these previous studies serve a fundamentally different purpose. Their idealized scenarios assume constant atmospheric conditions and assess how allowing those atmospheric conditions to change by air-sea coupling changes SST variability. Our study does not compare the effects of a static atmosphere to a coupled atmosphere. Our uncoupled atmosphere is dynamic, not static, since it is allowed to evolve and takes into account realistic lateral and surface forcings. In fact, we are comparing the effects of a one-directional atmosphere to a coupled (and co-evolving) atmosphere. The uncoupled atmosphere is one-directional in the sense that the atmosphere evolves due to momentum and heat fluxes from the 5 km run but then the resulting atmosphere is used to force 4 km ROMS. Our study addresses the impact of coupling from a pragmatic, modeling perspective. We investigate how modelled

SST variability changes when we replace a dynamic atmosphere that forces the ocean, with an atmosphere that co-evolves with the ocean.

Our answer is that coupling may not make a large difference if the goal is simply to create a model that is in phase with observations. The uncoupled model has slightly higher correlations with observations. However, correlation is an imperfect test of model proficiency, since it ignores the internal variability, which is randomly phased between the two models. Internal variability cannot be ignored since it is a significant fraction of the variability, especially farther from the coast. In fact, it could be the uncoupled model's tendency to underestimate the internal variability that leads to higher correlations, since there is less masking of the forced signal by randomly phased variations.

It is important to note that our definition of forced is domain dependent. In our model setup, the ocean domain is large enough that signals from the boundary conditions have time to be altered due to instabilities as they propagate to the interior of the domain. The inter-model correlations of SST are low ($r < 0.4$) for much of the open ocean (see Figure 8). However the domain is too small for much atmospheric internal variability to develop. For instance, the inter-model correlations of winds as 10m are extremely high ($r > 0.9$) for nearly the whole domain (figure not shown). Conversely, if the ocean domain were much smaller (e.g., covering only a narrow 20 km strip of ocean along the coast), there would be less space for eddies and other instabilities to be generated internally. Thus nearly all of the variability would be forced.

Because of our model domain is a size such that there is atmospheric forced signals are transmitted with little disruption, while oceanic forced signals masked by internal variability, we can conclude that SST variability near the coast that is shared between the models is likely caused by variability in the large scale atmospheric flow rather than remote ocean signals. Although some SST variability near the coast may be due to the lateral ocean boundary conditions, this fraction is small and appears to be not as significant on the intra-annual time scales studied here.

6 Summary

In this study we compared SST variability between the fully coupled UMCM model and a similar, but uncoupled model. Our goal was to see how including air-sea coupling would affect intra-annual SST variability in a realistic domain, using reanalysis boundary conditions (SODA and NARR) over the historical time period 1981-1990. We evaluated the quantity, phasing, and spatial patterns of SST variability by comparing the model output to ten NDBC buoys along the California coast.

We found that the amount of variability in the coupled model is closer to observed levels than for the uncoupled model. When we examined which model was in better phase agreement with observations, we found slightly higher correlations for the uncoupled model than for the coupled model. This may be due to the higher levels of internal variability in the coupled model which serve to mask the forced variability. The effect of coupling is the most dramatic when considering the spatial patterns of coherent variability. The coupled model has high correlations between distant locations, while correlations between points in the uncoupled model drop off quickly with distance. These correlations are too weak in the uncoupled model, while the coupled model's correlations are closer to observed values. Examining the coastal average (averaging over the ten buoy locations) showed that the largest differences in coherent variability are on longer time scales. On time scales longer than 120 days, the coupled model has more than twice as much coherent variability as the uncoupled model. Furthermore, on these longer time scales, the correlation between the models is lower, suggesting more internal variability on longer time scales. Thus the coupled model has much more total variability than the uncoupled model when there is more internal variability is present. This fits with our theory that coupling preferentially affects internal variability. This is due to the setup of our uncoupled model, which allows it to reproduce forced variability like a coupled model, but has reduced internal variability.

We conclude that adding air-sea coupling to a regional model may be necessary when trying to simulate realistic levels of variability. Models without coupling may have good correlations with observations because the reduced amount of internal variability prevents masking of the forced signal. The uncoupled model has enhanced the clarity of the forced signal, but at the cost of unrealistic levels of internal variability. Thus we recommend using coupling for modelling applications

where variability must be properly simulated.

7 References

Boé J., A. Hall, F. Colas, J. C. McWilliams, X. Qu, J. Kurian, S. B. Kapnick, H. Frenzel, 2010: What shapes mesoscale wind anomalies in coastal upwelling zones?. Clim Dyn, 36, 2037-2049, doi: 10.1007/s00382-011-1058-5.

Carton, J. A., B. S. Giese, 2008: A reanalysis of ocean climate using simple ocean data assimilation (SODA). Mon Weather Rev, 136, 2999–3017.

Capet, X. J., P. Marchesiello, J. C. McWilliams, 2004: Upwelling response to coastal wind profiles. Geophysical Research Letters, 32, L13311, doi:10.1029/2004GL020123.

Capet, X. J., F. Colas, J. C. McWilliams, P. Penven, and P. Marchesiello, 2008: Eddies in eastern boundary subtropical upwelling systems. Ocean Modeling in an Eddying Regime. Geophys Monogr Ser, 177, edited by M. W. Hecht and H. Hasumi, pp. 131–147, AGU, Washington, D. C., doi:10.1029/177GM10.

Chelton, D. B., and Coauthors, 2001: Observations of coupling between surface wind stress and sea surface temperature in the Eastern Tropical Pacific. J Clim, 14, 1479-1498.

Chen, F., J. Dudhia, 2001: Coupling an advanced land-surface/ hydrology model with the Penn State/NCAR MM5 modeling system. Part I: model description and implementation. Mon Weather Rev, 129, 569–585.

Creel, L., 2003: Ripple Effects: Population and coastal regions. Population Reference Bureau, Accessed 17th April 2012, www.prb.org

Crossett, K. M., T. J. Culliton, P. C. Wiley, T. R. Goodspeed. 2004. Population trends along the coastal United States: 1980-2008. NOAA/National Ocean Service. Accessed 17th April 2012, www.oceanservice.noaa.gov

Dong, C., J. C. McWilliams, A. Hall, M. Hughes, 2011: Numerical simulation of a synoptic event in the Southern California. J Geophys Res, 116, C05018, doi:10.1029/2010JC006578

Enriquez, A. G., C. A. Friehe, 1995: Effects of wind stress and wind stress curl variability on coastal upwelling. J Phys Oceanogr, 25, 1651–1671.

Hong, S. Y., Y. Noh, J. Dudhia, 2006: A new vertical diffusion package with an explicit treatment of entrainment processes. Mon Weather Rev, 134, 012318-2341.

Huyer, A. 1983: Coastal upwelling in the California Current System. Progress in Oceanography, 12, 259-284.

Jin, X., C. Dong, J. Kurian, J. C. McWilliams, D. B. Chelton, Z. Li, 2009: SST-wind interaction in coastal upwelling: oceanic simulation with empirical coupling. J Phys Oceanogr, 39(11), 2957-2970.

Maloney, E. D., D. B. Chelton, 2006: An assessment of the sea surface temperature influence on surface wind stress in numerical weather prediction and climate models. J Clim, 19(12), 2743–2762.

Marchesiello, P., J. C. McWilliams, A. Shchepetkin, 2003: Equilibrium structure and dynamics of the California Current System. J Phys Oceangr, 33, 753-783.

Mlawer, E., S. Taubman, P. Brown, M. Lacono, S. Clough, 1997: Radiative transfer for inhomogeneous atmosphere: RRTM, a validated correlated-k model for the longwave. J Geophys Res, 102, 16663–16682.

Perlin, N., E. D. Skyllingstad, R. M. Samelson, P. L. Barbour, 2007: Numerical simulation of air-aea coupling during coastal upwelling. J Phys Oceanogr, 37, 2081-2093.

Samelson, R. M., E. D. Skyllingstad, D. B. Chelton, S. K. Esbensen, L. W. ONeill, N. Thum, 2006: On the coupling of wind stress and sea surface temperature. J Clim, 19, 1557–1566.

Seo H., A. J. Miller, J. O. Road, 2007: The Scripps Coupled Ocean–Atmosphere Regional (SCOAR) model, with applications in the Eastern Pacific Sector. J Clim, 20, 381-402.

Shchepetkin, A. F., J. C. McWilliams, 2005: The regional oceanic modeling system (ROMS): a split-explicit, free-surface, topography-following-coordinate oceanic model. Ocean Model, 9, 347–404.

Shchepetkin, A. F., J. C. McWilliams, 2009: Correction and commentary for "Ocean forecasting in terrain-following coordinates: formulation and skill assessment of the Regional Ocean Modeling System" by Haidvogel et al. J Comp Phys, 227, 3595–3624.

Skamarock, W. C., et al., 2007: A description of the advanced research WRF version 2. NCAR/TN-468?STR. NCAR technical note.